Multistage evolution of intracontinental basins: the case of the Lusitanian Basin

Fernando Ornelas Marques[1], Diogo F.A. Gaspar[2], Julio Cesar Horta de Almeida[2], and Carlos R. Nogueira[3]

[1]Retired
[2]Universidade Estadual do Rio de Janeiro, Brasil
[3]University of Lisbon

March 9, 2023

Abstract

The Newfoundland-Iberia rift, which includes the Lusitanian Basin (LB), has been considered the archetype of a magma-poor rift, but its main steps are still debated. The new data reported here indicate that the LB's eastern border comprises two contrasting types of contact between continental sediments and Variscan basement: major angular unconformity and master bounding fault. The unconformable contact could mean a pre-rift sag basin, or a syn-rift half-graben with flexural boundary in the E. However, given that newly recognized master NW-SE to NNW-SSE bounding faults displace the red continental deposits and basal unconformity by hundreds of meters, we infer that the master bounding fault is Alpine and displaces the base of a previous sag basin. In the case of unconformable contact and sag basin, the age of the red continental deposits would be older than the currently attributed Late Triassic age, and represent the missing Late Variscan denudation molasse. It seems therefore that the LB could be a rift basin underlain by an older and smaller sag basin. Later, Pangaea rifting produced a full graben, the LB, bounded to the east by a newly mapped master fault reactivating a major Variscan shear zone in the northern half of the Lusitanian Basin. A similar development of composite basins can be found in NE Brazil, where some Mesozoic intracontinental basins also show evidence of two-stage basin formation, an early sag (Palaeozoic) and a later rift (Mesozoic).

Hosted file

958035_0_art_file_10779615_rr7nj0.docx available at https://authorea.com/users/57673/articles/628677-multistage-evolution-of-intracontinental-basins-the-case-of-the-lusitanian-basin

Multistage evolution of intracontinental basins: the case of the Lusitanian Basin

D.F.A. Gaspar[a], F.O. Marques[*], J.H. Almeida[b], C.R. Nogueira[c]

[a] PPGABFM, Faculdade de Geologia – UERJ, Rio de Janeiro - RJ - CEP 20550-900, Brazil

[b] Tektos- UERJ, Rio de Janeiro - RJ - CEP 20550-900, Brazil

[c] Universidade de Lisboa, Edifício C6, Piso 2, 1749-016, Lisboa, Portugal

[*] Corresponding author

Abstract

The Newfoundland-Iberia rift, which includes the Lusitanian Basin (LB), has been considered the archetype of a magma-poor rift, but its main steps are still debated. The new data reported here indicate that the LB's eastern border comprises two contrasting types of contact between continental sediments and Variscan basement: major angular unconformity and master bounding fault. The unconformable contact could mean a pre-rift sag basin, or a syn-rift half-graben with flexural boundary in the E. However, given that newly recognized master NW-SE to NNW-SSE bounding faults displace the red continental deposits and basal unconformity by hundreds of meters, we infer that the master bounding fault is Alpine and displaces the base of a previous sag basin. In the case of unconformable contact and sag basin, the age of the red continental deposits would be older than the currently attributed Late Triassic age, and represent the missing Late Variscan denudation molasse. It seems therefore that the LB could be a rift basin underlain by an older and smaller sag basin. Later, Pangaea rifting produced a full graben, the LB, bounded to the east by a newly mapped master fault reactivating a major Variscan shear zone in the northern half of the Lusitanian Basin. A similar development of composite basins can be found in NE Brazil, where some Mesozoic intracontinental basins also show evidence of two-stage basin

formation, an early sag (Palaeozoic) and a later rift (Mesozoic).

Keywords: Lusitanian Basin; composite basin; sag basin or half-graben; Triassic sediments; debris-flow dominated fans; unconformable or fault basin-basement contact

1. Introduction

Intracontinental sedimentary basins may reflect the complex history of the basement where they sit. For instance, the same basin can comprise sediments from two tectonic cycles: the older sediments, deposited in a sag basin, can be the witness of denudation in the post-collisional, waning stages of an orogen; the younger sediments can be deposited in a subsequent rifting episode representing the beginning of a new tectonic cycle. This could be the case of the intracontinental basins in NE Brazil, where Palaeozoic sag basin sediments precede Mesozoic rift-related sediments. Here we propose a similar evolution for the Newfoundland-Iberia Rift, where Late Variscan (Permian) sag basin sediments could precede Mesozoic rift-related sediments.

The Lusitanian Basin (LB) is the eastern expression of the Newfoundland-Iberia Rift (Fig. 1). The present-day LB shows an approximate NNE-SSW direction, concave to the WNW (Fig. 1). The northern half grossly follows the NNW-SSE to N-S Porto-Tomar Shear Zone (PTSZ), and the southern half strikes approximately NNE-SSW, the direction of a well-known late-Variscan fault system (e.g. Arthaud and Matte, 1977; Marques et al., 2002). This means that the LB's eastern boundary corresponds to reactivated major shear zones inherited from the Palaeozoic Variscan orogeny. The LB was filled in the early stages by continental red conglomerates and sandstones attributed to the Late Triassic (< 230 Ma), which were sub-divided by Palain (1976) into (from bottom to top) sequences A, B and C (each sub-divided into A1 and A2, B1 and B2, and C1 and C2). Together, these sediments are known as the Silves Group. This Late Triassic sedimentation was followed by the deposition of thick evaporites in the earliest Jurassic (ca. 200 Ma), concomitant with the CAMP magmatism (Central Atlantic Magmatic Province), then followed by a thick Jurassic marine carbonate sequence (ca. 195 to 150 Ma), and finally by siliciclastic continental deposits from the Late Kimmeridgian (ca. 150 Ma) to present-day, with a major unconformity at the Jurassic-Cretaceous boundary (ca. 145 Ma) and intercalated marine deposits in the Cenomanian-Turonian and Miocene.

Despite having been studied since the late nineteenth century, the LB is yet not well understood regarding onshore boundary master faults, continental rifting characteristics, and geodynamic meaning of the earliest red siliciclastic deposits. Previous work has suggested that the LB's eastern boundary is flexural (eastern border of a half-graben), where small faults define a horst-graben architecture, and no field evidence for a master bounding fault has been shown in the literature (e.g. Wilson et al., 1989; Azeredo et al., 2003; Kullberg et al., 2006; Soares et al., 2012). These works show field evidence of faults with very small displacement, all of them cutting the Silves Group itself, not the master bounding fault separating the LB (hanging wall) from the Variscan basement (footwall). To our knowledge, all previous work has concentrated either on small areas or on a very limited number of data points within the Silves Group to infer rift kinematics, and none has proposed a geodynamic interpretation for the red siliciclastic deposits and rifting based on widespread field data with hundreds of outcrops analysed as we did in the present work. Here we seek to better understand the significance of the red siliciclastic deposits in the LB, especially its age and tectonic meaning, and bring new answers and views regarding late- to post-Variscan Permo-Triassic tectonics. The age of the lowermost siliciclastic sediments in the LB is not known, because they have not been dated, mostly because fossils like palynomorphs could not be found in the A1 unit defined by Palain (1976) (Vilas Boas et al., 2021). Soares et al. (2012) suggested the existence of a "proto-Lusitanian Basin" forming at ca. 245 Ma (earliest Middle Triassic). In contrast to our interpretation reported here (sag basin due to collapse of the Variscan orogen), Soares et al. (2012) proposed that the "proto-Lusitanian Basin" formed by extensional tectonics during migration of the Neotethys to the west.

In order to accomplish our objectives, we carried out structural/tectonic work along the LB's eastern boundary in its northern half, not only where the red siliciclastic deposits have been previously mapped but also to the east inside the Variscan basement where the main fault or faults have not been mapped but should exist.

2. Geological Setting

The Triassic rifting in the early stages of the LB was mostly controlled by lithospheric-scale faults inherited from the late stages of the Variscan orogeny (310 to 270 Ma; Dias et al., 1998; Neiva et al., 2012; Martínez Catalán et al., 2014; Valle Aguado et al., 2017). This late-Variscan episode produced two main conjugate strike–slip fault systems in Iberia (Marques et al., 2002): the NNE system (e.g. Vilariça and Chaves faults), dextral during the Variscan and sinistral during the Alpine (Marques et al., 2002), and the conjugate ENE-WSW sinistral system (e.g. the faults reactivated in the Alpine orogeny to form the ENE-WSW Serra da Estrela pop-up and the Spanish Central System) (Marques et al., 2002). Earlier in the Variscan orogeny, NNW shear zones formed that were initially ductile and later brittle.

A synthesis published by Kullberg et al. (2006) proposed that the LB has undergone four rifting episodes. In the synthesis paper of Leg 210 of the Ocean Drilling Project, Tucholke and Sibuet (2007) divided the LB evolution into two phases: the first phase (Late Triassic to Early Jurassic) is characterized by a broad continental rift without separation, and the second stage by three rifting episodes (Fig. 2). Pena dos Reis et al. (2010) considered that three rifting and two "Sag" episodes have occurred during the LB's evolution (Fig. 2). Based on large unconformities and new AFT data, Barbarand et al. (2021) proposed the existence of only two continental rift stages, one (Rift 1) from the Late Triassic to the latest Jurassic (ca. 150 Ma), and the other (Rift 2) between the Jurassic/Cretaceous boundary (ca. 145 Ma) and the first formation of basaltic oceanic crust at ca. 110 Ma. This rift-to-drift stage marks the shift from continental to oceanic rifting, which can be considered Rift 3 lasting until present-day. The period of interest in our work is the beginning of the first phase in the Triassic or earlier.

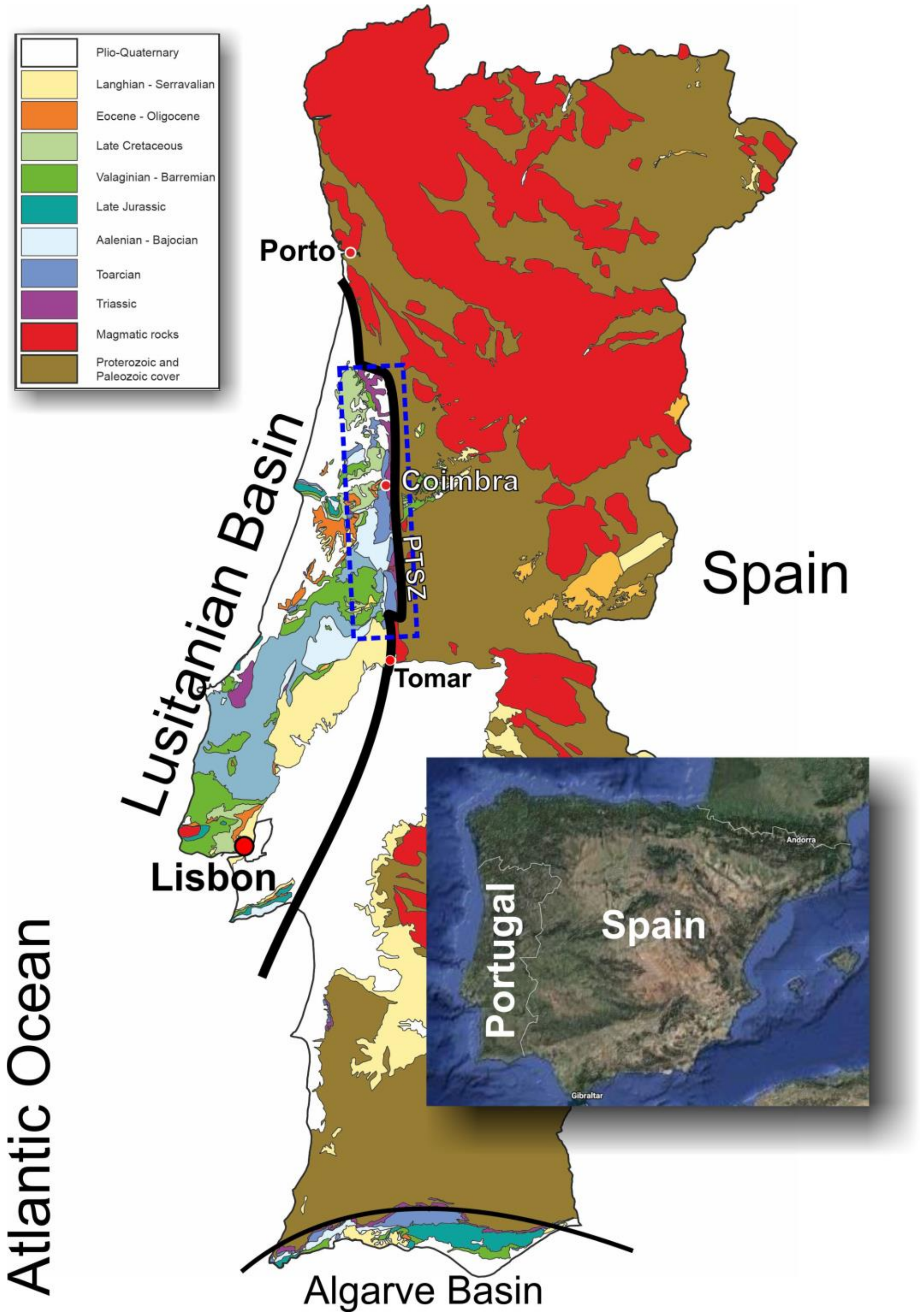

Figure 1. Simplified geological map for location of the study area (dashed blue rectangle) and main tectonic structures in the Lusitanian Basin. Image on inset at bottom right from Google Earth.

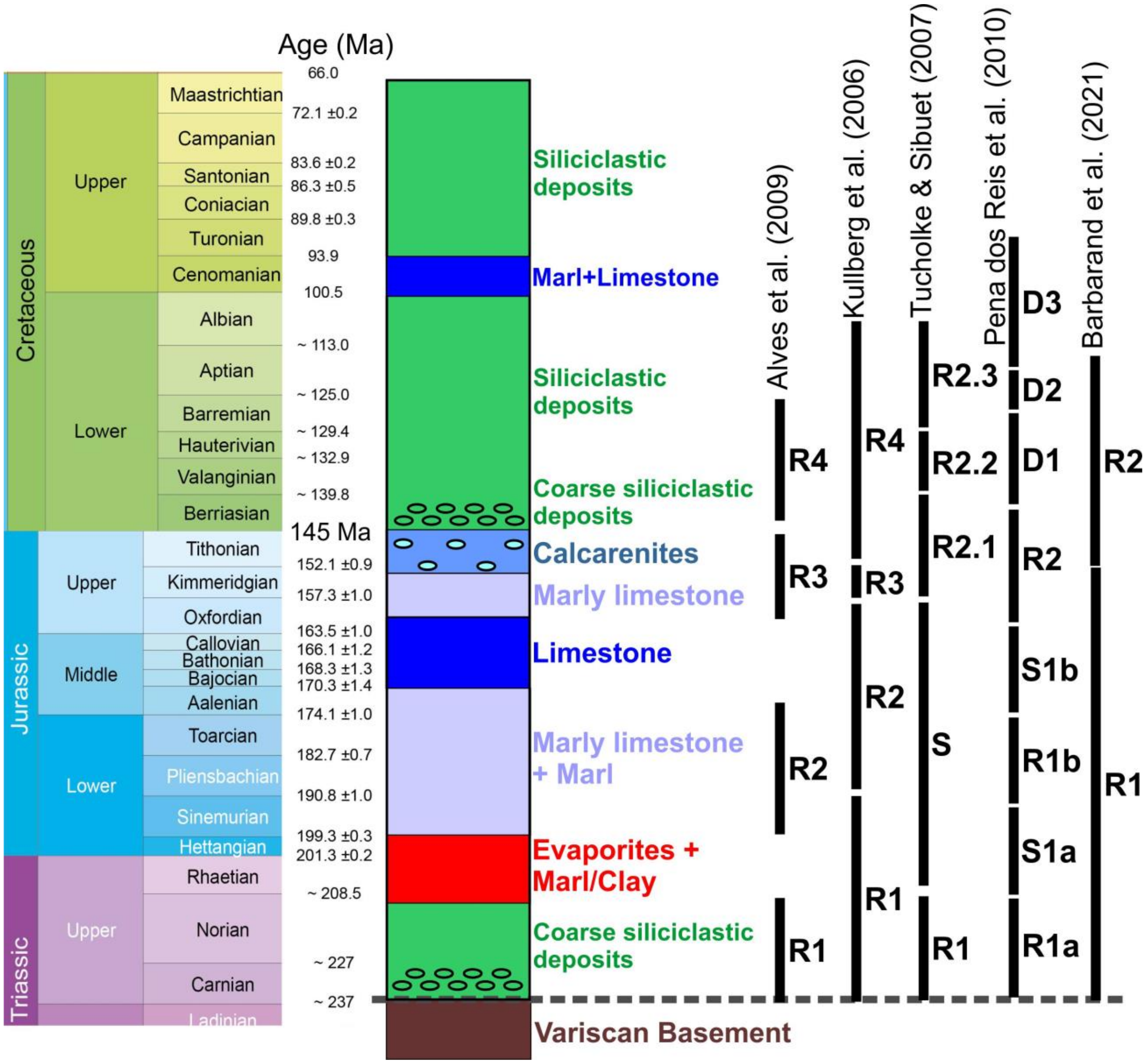

Figure 2. Synthetic lithostratigraphic chart for the LB (left), and different phases of the LB's tectonic evolution (right) showing rift (R), sag (S) and drift (D) stages according to the indicated authors.

The Silves Group in the LB have been divided into several major units (see Table 1), which together comprise the Grés de Silves Group (e.g. Choffat, 1882, 1903-1904; Palain, 1976). The first rift sediments (Conraria Formation), which are the main object of this work, are composed of coarse red sandstones and conglomerates, and more rarely grey and red pelitic beds. The clasts are composed of basement-derived metamorphic and igneous rocks, and the clast size decreases away from the master bounding fault. The depositional environment of these sediments away from the

Porto-Tomar Fault (master bounding fault) has been considered an intermittent alluvial system with low-sinuosity braided channels (e.g. Soares et al., 2012). In the present work, we show that the facies variations are related to the proximity to the Porto-Tomar Fault and the local dynamics of the fluvial system; therefore, it does not seem realistic to define a true stratigraphic subdivision of the Conraria Formation.

Table 1. Lithostratigraphic units of the Grés de Silves Group. A, B and C are megasequences, each with two sub-divisions. U – unconformities (U0, U1 and U2b – angular unconformities). Ages from Vilas-Boas et al. (2021).

<table>
<tr><th>Age</th><th colspan="3">Palain (1976)</th><th colspan="2">Soares et al. (2012)</th></tr>
<tr><td rowspan="3">Hettangian</td><td rowspan="3">C</td><td>C2</td><td></td><td rowspan="12">Grés de Silves Group</td><td rowspan="4">Pereiros Formation</td></tr>
<tr><td></td><td>U3b</td></tr>
<tr><td>C1</td><td></td></tr>
<tr><td rowspan="5">Rhaetian</td><td rowspan="5">B</td><td>B2</td><td></td></tr>
<tr><td></td><td>U3a</td><td rowspan="2">Castelo Viegas Formation</td></tr>
<tr><td rowspan="3">B1</td><td></td></tr>
<tr><td>U2b</td><td></td></tr>
<tr><td></td><td>Penela Formation</td></tr>
<tr><td></td><td></td><td></td><td>U2a</td><td></td></tr>
<tr><td>Norian</td><td rowspan="2">A</td><td>A2</td><td></td><td rowspan="2">Conraria Formation</td></tr>
<tr><td>?</td><td>A1</td><td></td></tr>
<tr><td></td><td></td><td></td><td>U1</td><td></td></tr>
<tr><td colspan="6">Buçaco Basin</td></tr>
<tr><td colspan="6">U0</td></tr>
<tr><td colspan="6">Variscan Basement</td></tr>
</table>

The Grés de Silves Group has been dated using palynomorphs (Doubinger et al., 1970; Adloff et al., 1974; Díez, 2000; Arche and López-Gómez, 2014; Vilas-Boas et al., 2021). A mid-Norian (ca. 220 Ma) to earliest Rhaetian (ca. 207 Ma), age was attributed to the A2 member of the Conraria Formation (Vilas-Boas et al., 2021). This means that the A1 member (ca. 120 m thick) was not date and, therefore, its age is still unknown. A Middle Carnian (ca. 232 Ma) to Upper Norian (ca. 215 Ma) age has been inferred for the Castelo Viegas Formation (Adloff et al., 1974; Díez, 2000; Arche and López-Gómez, 2014), but Vilas-Boas et al. (2021) could not find material appropriate for dating. Adloff et al. (1974) proposed an Hetangian – Sinemurian age (ca. 201-191 Ma) for the base of the Pereiros Formation, i.e. term C1 of Palain (1976). However, Díez (2000) proposed a Lower Norian to Rhaetian age for the term C1. More recently, Vilas-Boas et al. (2021) inferred an uppermost Rhaetian and Hettangian age for the Pereiros Formation.

The basement units below the LB in the study area are (Oliveira et al., 1992; Soares et al., 2007): the Upper Proterozoic Série Negra mostly composed of black shale and greywacke; the Upper Proterozoic Beiras Group characterized by thick layers of metagraywackes; and the Ordovician Armorican Quartzites (mostly quartzite and shale). The relationship between the lowermost red siliciclastic deposits and the underlying sediments of the Buçaco Basin is not clear, but it has been described as an angular unconformity (Domingos et al., 1983). The Buçaco Basin is mainly composed of breccia, siltstone, mudstone, conglomerate and coal seams, and the age is Permo-Carboniferous as inferred from palynomorphs (Machado et al., 2018).

3. Field data

The study of the Conraria Formation comprised several challenges. Most outcrops have small dimensions and are sparsely distributed, hence we had to analyse a large number of outcrops in order to consistently integrate the results for the whole study area. We collected sedimentary and structural data on 368 outcrops. These outcrops are located along the eastern margin of the LB (Fig. 3), not only where the red siliciclastic deposits are recognized on geological maps, but also to the east, in the basement adjacent to the basin (Fig. 3), where we suspected that red conglomerates and sandstones should be found if the LB were bounded to the east by master faults.

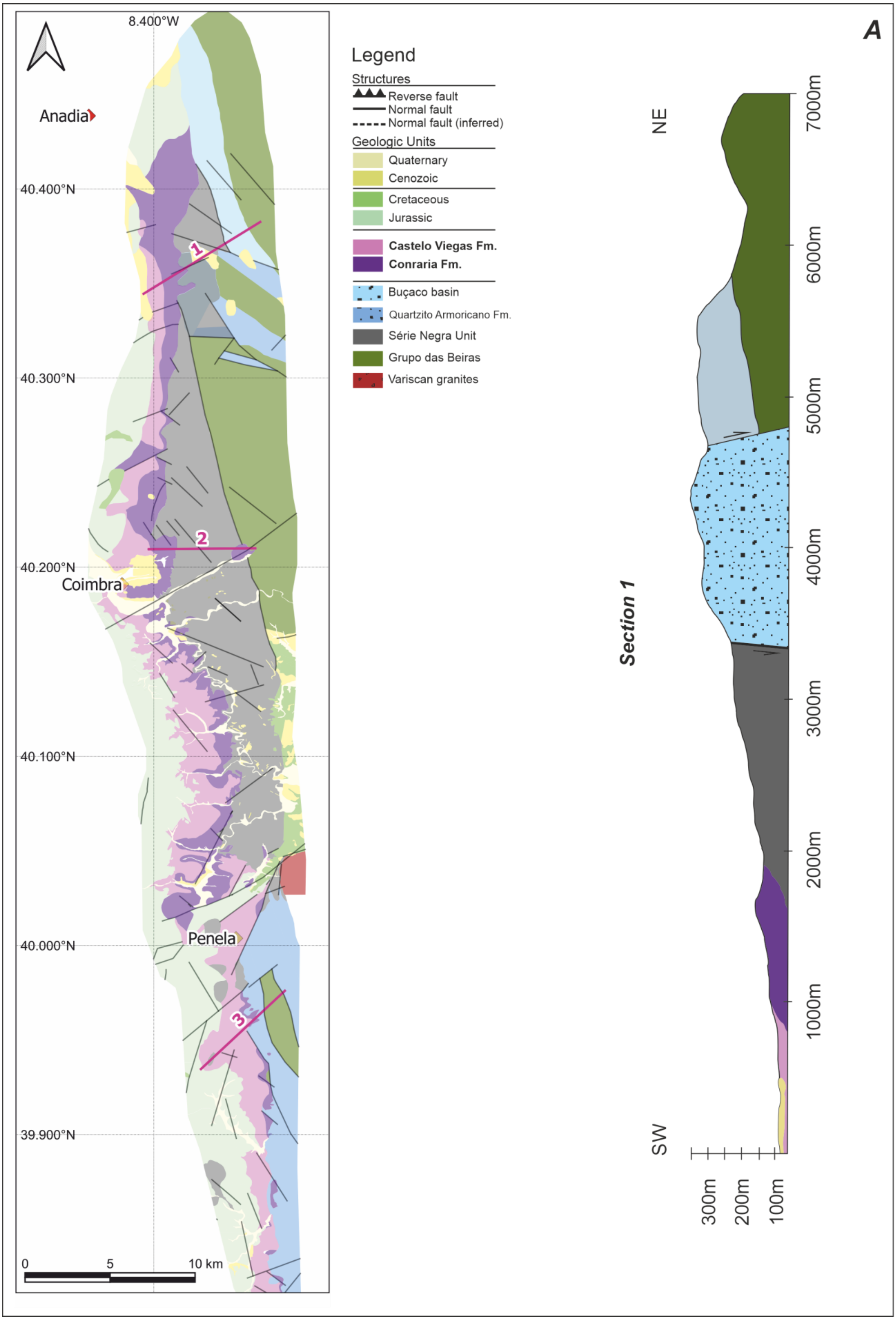
A
8.400°W
Anadia
40.400°N
40.300°N
40.200°N
40.100°N
40.000°N
39.900°N
Coimbra
Penela
1
2
3
0
5
10 km
Legend
Structures
Reverse fault
Normal fault
Normal fault (inferred)
Geologic Units
Quaternary
Cenozoic
Cretaceous
Jurassic
Castelo Viegas Fm.
Conraria Fm.
Buçaco basin
Quartzito Armoricano Fm.
Série Negra Unit
Grupo das Beiras
Variscan granites
Section 1
NE
SW
7000m
6000m
5000m
4000m
3000m
2000m
1000m
300m
200m
100m

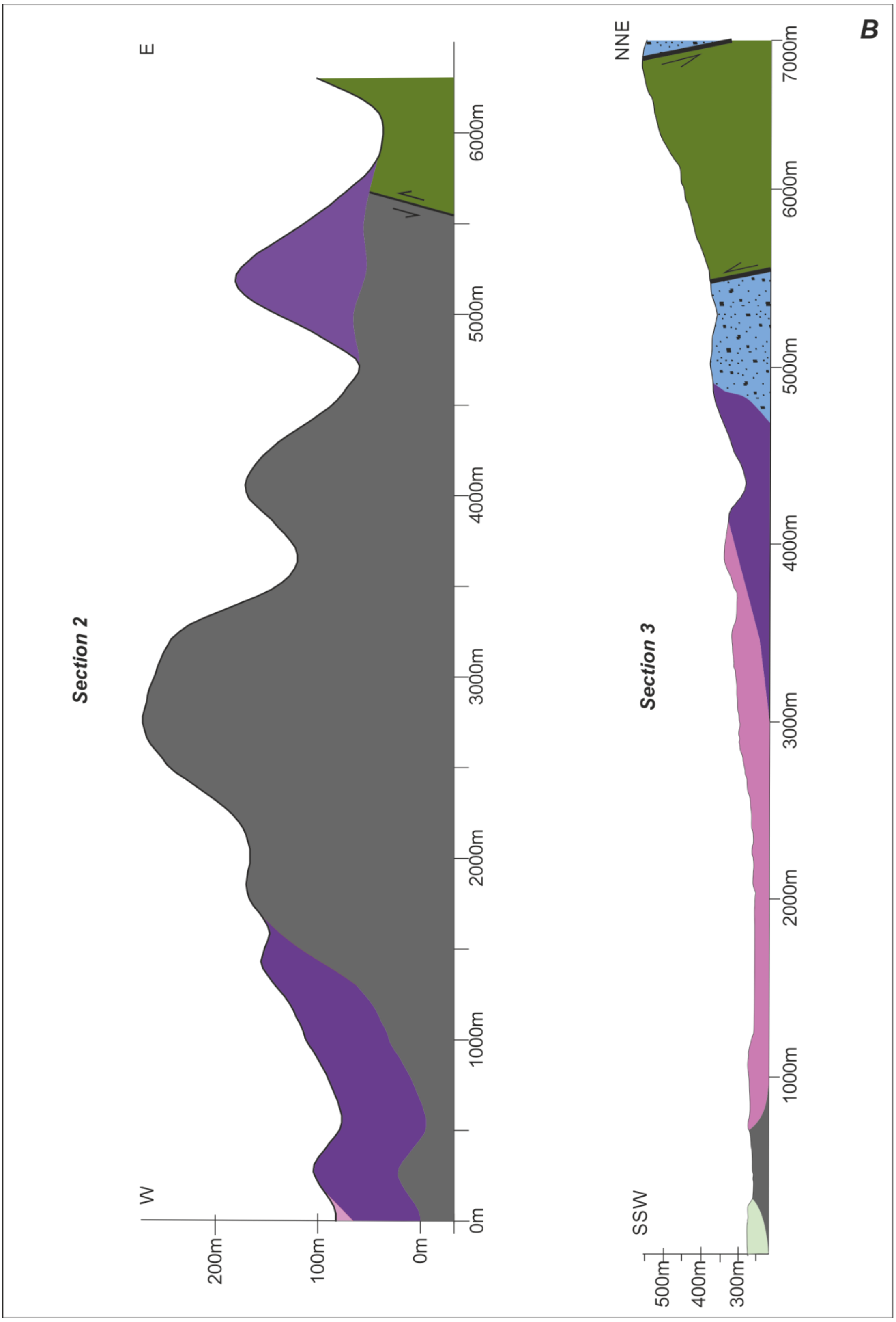

Figure 3. A) Geological map and cross-sections of the study area. This map encompasses the data collected for this work, and uses as a base the available 1:500,000 and 1:50,000 geological maps (Oliveira et al., 1992; Soares et al., 2007). B) Cross-sections detailing the easternmost sections of the Coimbra Basin and its contact with the basement. Note the Conraria Formation outcropping at different altitudes.

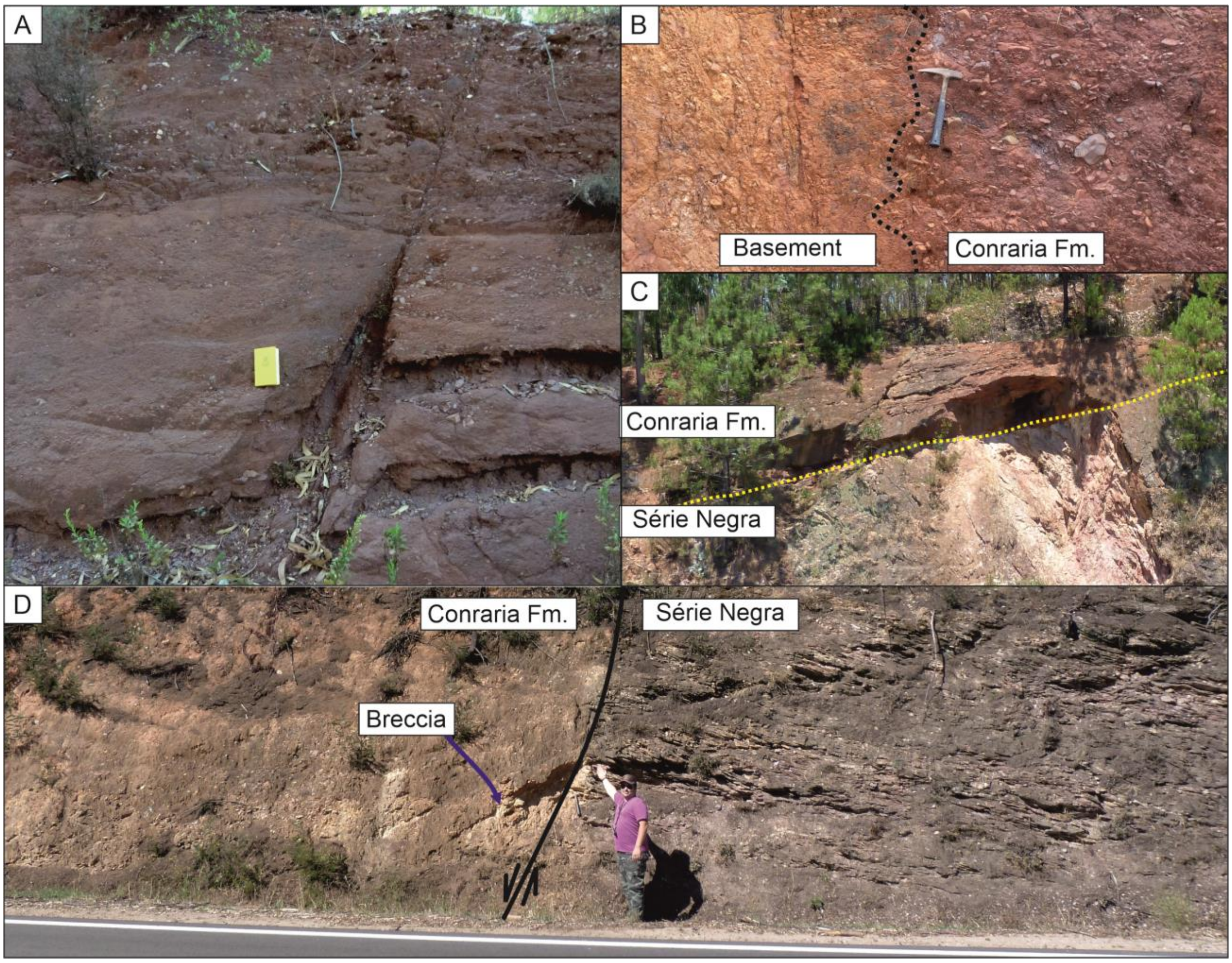

Figure 4. Examples of synsedimentary faults (A) and contact between basement and red siliciclastic sediments (B to D). (B) Example of contact by fault scarp (dotted line to the left of the hammer); (C) outcrop with an example of contact through unconformity (yellow dotted line); and (D) example of fault contact.

The outcrops were located using GPS and 1:25,000 topographic maps. In each outcrop we indexed all the structures, such as faults, fractures, foliation, bedding, etc. We also recorded the sedimentary features using Miall's (1996) concepts. Qualitative and quantitative analyses of deformation were carried out, including the determination of the stress field by the right dihedral method of Angelier and Mechler (1977). The determination of the relative movement of the fault blocks was done through kinematic characterization of the indicators on fault planes (Angelier, 1994). We used the Win-Tensor 4 software (Delvaux, 2012) for the computer-assisted calculation of fault kinematics and stress fields. This software enables the creation of theoretical striae for the faults in which no striae were observed in the field. However, we followed the principle proposed by Angelier (1989) in which α should be at most 22º.

Another challenge presented by the Conraria Formation is that this unit was later affected by other rift phases and Alpine deformation; therefore, we had to discriminate between syn- and post-sedimentary structures. We used criteria based on the premises that faults propagate upwards, sedimentation is a discontinuous process, and the classical principle of superposition. For instance, a fault affecting Conraria sediments and covered by the same unit was active only during the deposition of the Conraria Formation (Fig. 4A).

3.1. Contact between red siliciclastic deposits and the Variscan basement

The red siliciclastic sediments contact directly with the basement through three main types of surface: unconformity, fault, and fault scarp (Figs. 4B, C and D). Fig. 4B shows the contact through a fault scarp, where the fault is concealed by the overlying coarse sediments deposited while the fault was inactive. In this case, the fault ceased activity leading to erosion of its scarp and deposition of red siliciclastic deposits. This type of contact can be identified by the absence of a clear fault surface and fault rock. Interestingly, in this type of contact the basement is Black Schist and the clasts comprising the sedimentary deposit are of quartzite and quartz eroded from topographic highs further away to the east. In Fig. 4C we can see an example of contact by an angular unconformity, where the red sediments are deposited on an erosional surface atop the Variscan basement. The fault contacts are characterized by syn-sedimentary faults and fault rocks that separate the Conraria sediments from the basement. The example in Fig. 4D is particularly representative of this type of contact. In this case, the red siliciclastic deposits to the left of the fault contain lithoclasts of the adjacent basement (black shale), which can be seen in the footwall. In this example we can observe a sedimentary breccia associated with the fault and deposited above the red conglomerate, thus indicating that, in this case, the fault was reactivated after a period of inactivity when the red conglomerate was deposited. The basement unit making up all the contacts is the Série Negra Formation (black schist with quartz veins), except one outcrop where the basement unit was the Armorican Quartzite (Fig. 3B, Sections 4 and 5).

Despite the different types of contact, several characteristics are similar in all outcrops where the basement is in direct contact with the Conraria Formation. The absence of large volumes of sedimentary breccia, the lack of clasts larger than cobbles, and, even in the contacts through fault, the source rock of most sediments is not from the adjacent basement unit. In only a few outcrops we have observed large granite boulders (e.g. inside the city of Coimbra, close to the contact with the Porto-Tomar Fault), and schist clasts in the vicinity of syn-sedimentary faults, but no further than 2 m from it.

3.2. Sedimentary data

The Conraria Formation comprises three facies, although the discontinuity of the outcrops hinders the full understanding of the vertical and horizontal distribution of each facies. Facies 1 comprises well-sorted coarse sand with dispersed sub-angular gravel (Fig. 5A). Commonly, this facies presents planar crossbedding, through crossbedding with set thickness ranging from 0,1 m to 1 m with trough-shaped bedding surfaces eroding underlying strata. These deposits define channel fills with a large range of dimensions, from 1 m to tens of meters wide and deep. Facies 1 is often interstratified with Facies 2 (Fig. 5A).

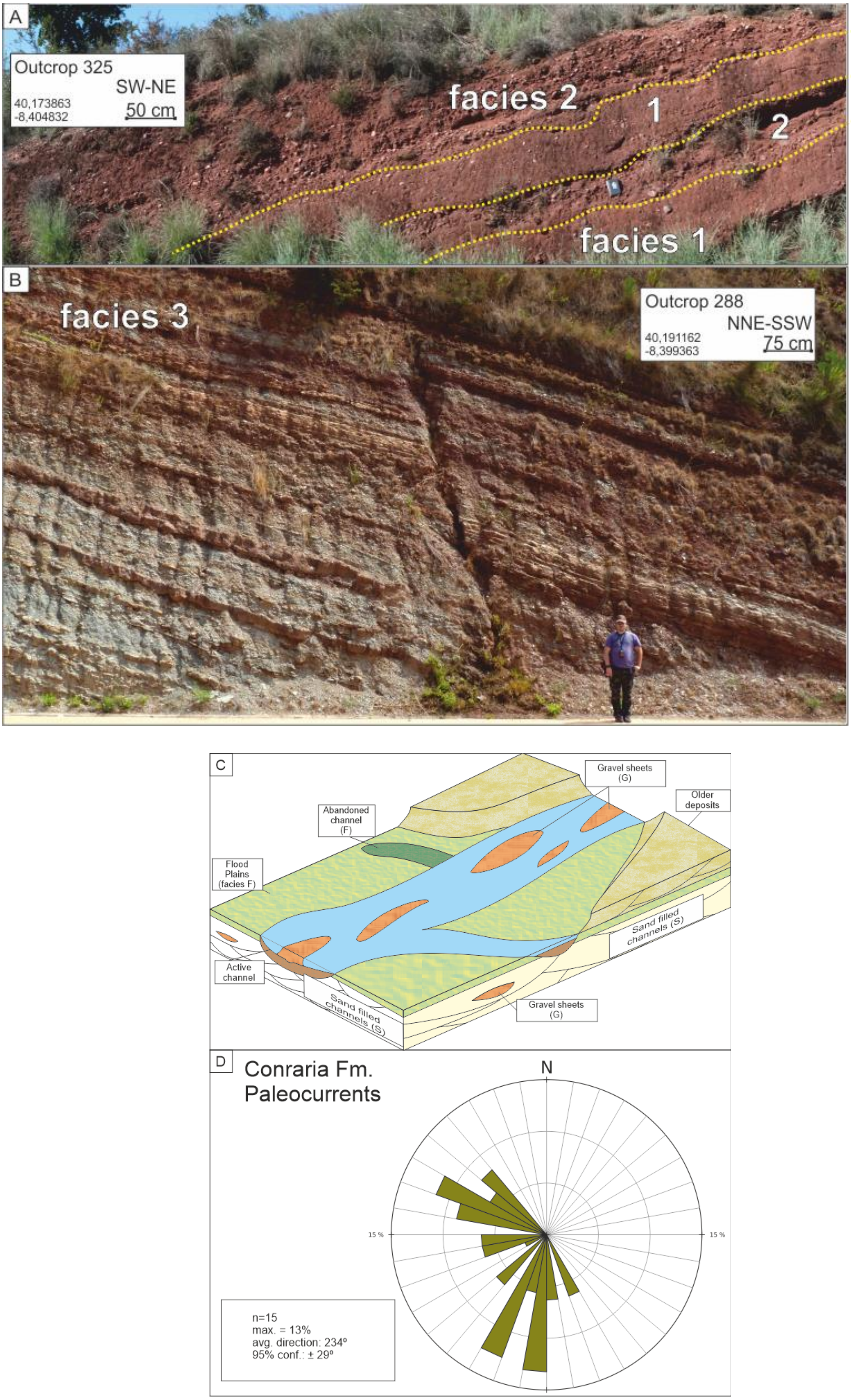
A
Outcrop 325
SW-NE
40,173863
-8,404832
50 cm
facies 2
1
2
facies 1
B
facies 3
Outcrop 288
NNE-SSW
40,191162
-8,399363
75 cm
C
Gravel sheets
(G)
Older
deposits
Abandoned
channel
(F)
Flood
Plains
(facies F)
Sand filled
channels (S)
Active
channel
Sand filled
channels (S)
Gravel sheets
(G)
D
Conraria Fm.
Paleocurrents
N
15 %
15 %
n=15
max. = 13%
avg. direction: 234º
95% conf.: ± 29º

Figure 5. Examples of the different lithofacies of the Conraria Formation: (A) Outcrop photo showing interbedded Facies 1 and 2. (B) Outcrop photo of Facies 3. (C) Schematic diagram of a gravel-bed braided alluvial system with sediment-gravity-flow deposits (after Miall, 1996). Note the contemporary deposition of all Conraria sedimentary facies. (D) Rose diagram of the Conraria Formation paleocurrents.

Facies 2 consists of sheets of matrix-supported quartzite pebbles to cobbles, where the clasts are moderate- to well-sorted and well-rounded (Fig. 5A). This facies typically does not display apparent stratification, other than crude bedding evidenced by particle size differentiation. Facies 3 is defined by laminated red sand and white silt deposits, and bedding thickness varies from 1 to 20 cm. Rare undulating bedding and root marks can be observed, although commonly this facies is arranged as planar bedding (Fig. 5B).

Facies 1 can be interpreted as filling of thalweg channels (Fig. 5C). Facies 2 can be interpreted to be a remnant of low-amplitude unit bars, recording abrupt introduction of large volumes of sediments, probably due to tectonic instability. Facies 3 can be interpreted as shallow deposits during final filling of the channel, and paedogenic characteristics indicate channel abandonment or overbank deposition. Therefore, facies associations 1, 2 and 3 can be interpreted as part of a gravel-bed braided alluvial system with sediment-gravity-flow deposits (*senso* Miall, 1996), and not individual stratigraphic units.

The Conraria Formation depositional environment was, presumably, a very dynamic system with relative low transport capability, when compared with fluvial systems established in the proximities of rift master bounding faults (Miall, 1996; Einsele, 2000) and periods of high transport capability. This conclusion is supported by the observation of several outcrops where the channels are restricted by gravel bars, together with the grain size (medium to coarse sandstones), sedimentary structures (absence of ripple marks), and the geometry of the deposits (presence of erosional surfaces between channels).

Paleocurrent data measured in the study area indicate current direction mainly to the SW.

These results are consistent with the paleocurrent control by the geometry of syn-rift faults presented in section 3.3.

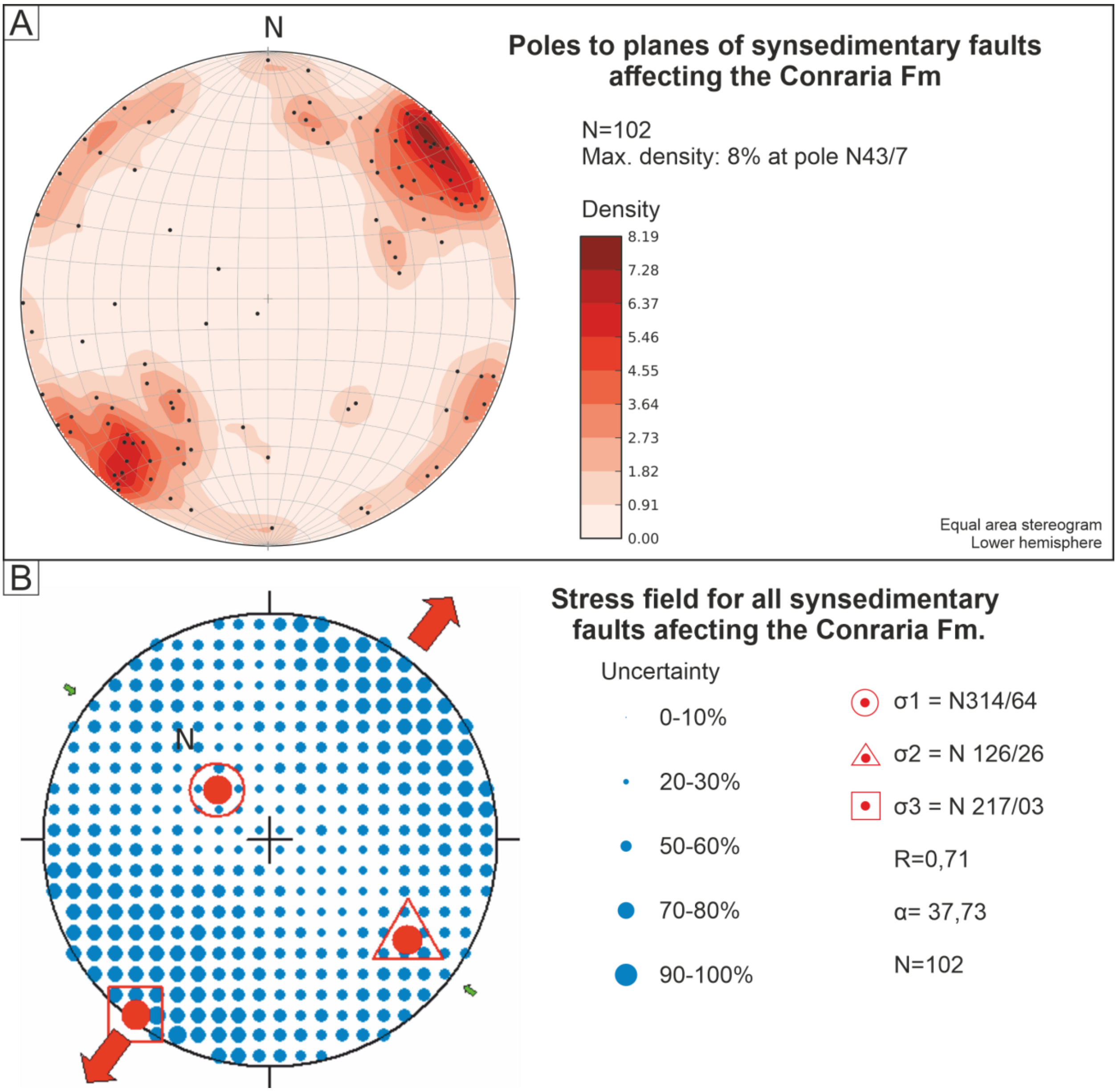

Figure 6. (A) Contoured maps of poles to planes of the Conraria Formation synsedimentary faults separated in two main sets, NW-SE and NNE-SSW. (B) Stereographic projection of all synsedimentary faults with stress tensor projection. (C) Stereographic projection of the recorded Triassic fault striations. (D) Stereographic projection of the tensors resulting from synsedimentary faults of the NW-SE set. (E) Stereographic projection of the tensors resulting from synsedimentary faults of the NNE-SSW set. Stress inversion of the fault-slip data was carried out using the right-dihedral method of Angelier and Mechler (1977) and WinTensor software. Note that to keep α value lower than 22º, 44 faults were disregarded. Red arrows represent extension, and blue arrows represent contraction.

3.3. Structural/tectonic data

On 126 Conraria outcrops, we measured 272 faults, 102 of which are most likely synsedimentary (Fig. 6A), but we were unable to determine if the remainder of the observed faults are synsedimentary or younger. In most cases, the fault vertical throw is < 1 m. On outcrop, the faults are generally curvilinear, spaced, and with a homogeneous distribution throughout the outcrop. The Conraria synsedimentary faults can be organized into two main sets: a more common NW-SE, and a less common NNE-SSW. In both cases, most faults dip steeply (around 70-80º), more than the typical normal fault (around 60º). A third minor set of faults also occurs, which strikes WNW-ESE and dips approximately 60º (Fig. 6A). The main kinematic criteria used were fault striations and bed displacement, although fault striations are quite rare due to the lithological characteristics of the sediments. When present, kinematic indicators allow inferring normal (dominant) oblique movement.

In order to determine the stress field during deposition of the Conraria Formation, we used only the synsedimentary faults and the method proposed by Angelier (1989) (Fig. 6B).

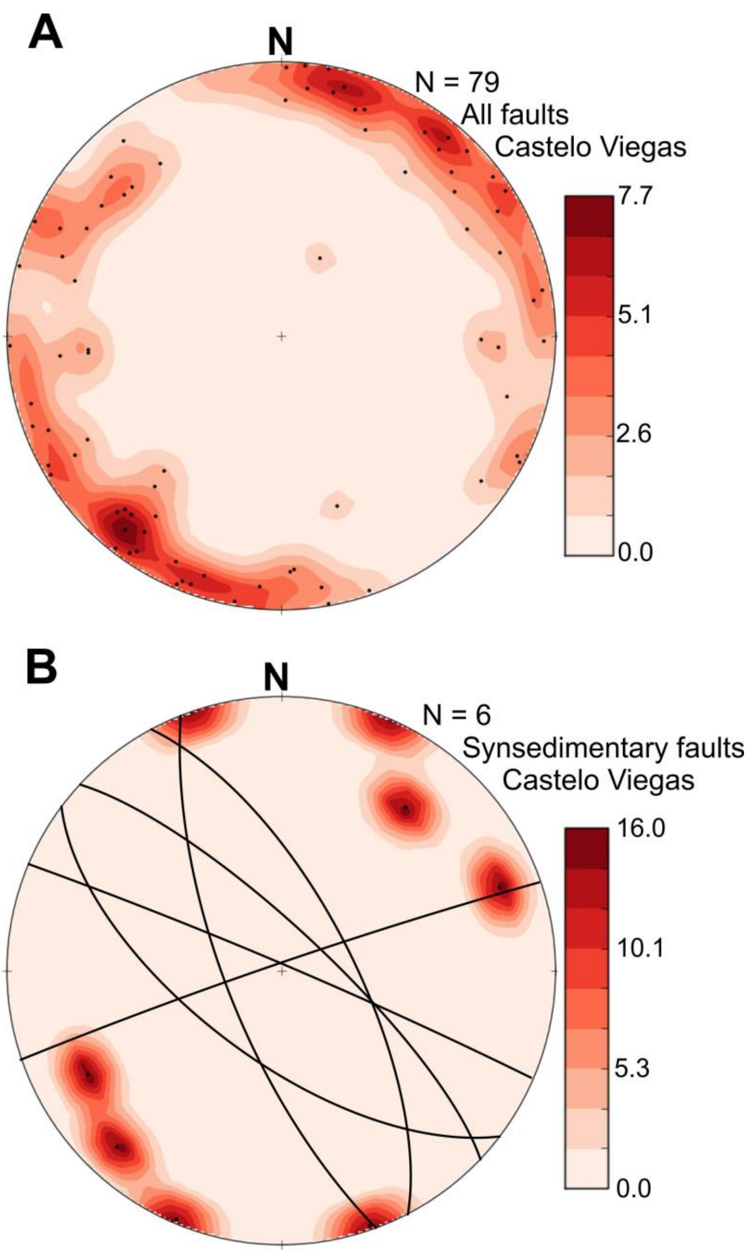

Figure 7. Equal-area, lower hemisphere projections of poles to planes using Fisher distribution. A – total of measured faults in the Castelo Viegas Formation. Note that most faults trend NW-SE, some trend NNE-SSW, and a few trend N-S. B – five synsediemntary faults trending around NW-SE, and one ENE-WSW. Despite some scattering, there are two preferential fault trends: around NW-SSE, parallel to the main tectonic trend in the basement, and ca. NNE-SSW, parallel to a well-known late-Variscan fault system (Marques et al., 2002), mainly represented by the Vilariça-Manteigas and Chaves-Régua faults.

The data collected in the younger Castelo Viegas Formation indicates an anti-clockwise rotation of the overall tectonic stress field, with synsedimentary faults trending NNE-SSW and a vertical sigma 1 orientated N126/72 (ENE-WSW). This NNE-SSW trend is present on the

Conraria Formation representing 42% of the non-synsedimentary faults recorded in this unit.

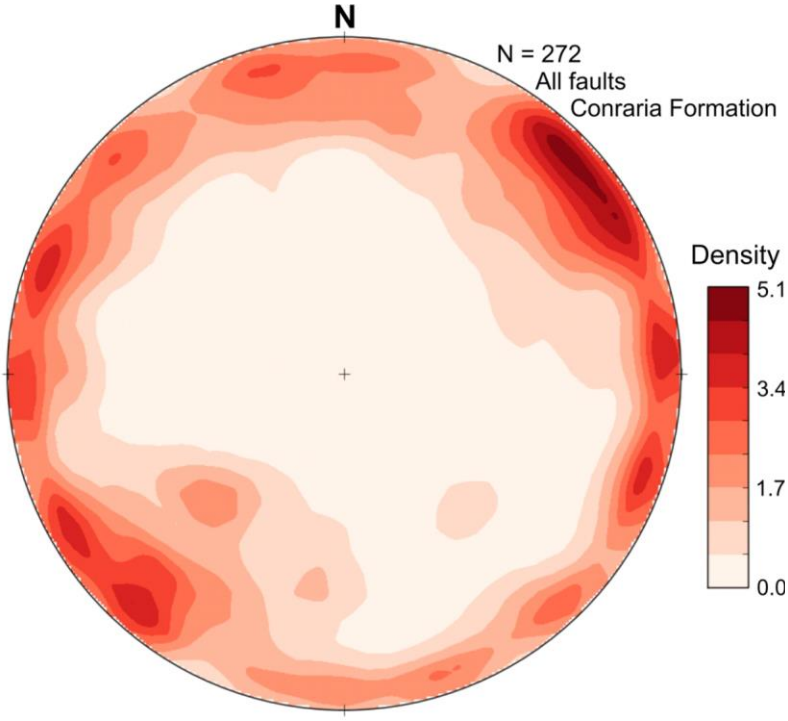

Figure 8. Equal-area, lower hemisphere projection of poles to planes using Fisher distribution. 272 measured faults in the Conraria Formation. Note that there are faults in all directions, although extension during rifting be commonly assumed as E-W. Despite scattering, there are preferential fault trends, as discussed in the main text.

4. Discussion

4.1. Ages of the studied sediments

All palynological studies carried out in the Silves Group (Adloff et al., 1974; Doubinger et al., 1970; Díez, 2000; Vilas-Boas et al., 2021) agree that the age of the sediments is Late Triassic (Norian-Rhaetian) to Early Jurassic (Hettangian). However, the base of the Conraria Formation (base of the Silves Group), i.e. its first 120 m, has never been dated.

Soares et al. (2012) overlooked the palynomorph ages (e.g. Adloff et al., 1974; Doubinger et al., 1970; Díez, 2000) and said that Castelo Viegas, the third formation from the bottom (above unconformity D2b), is the first formation at the base of the Lusitanian Basin. If it is already extensional and due to the propagation of the Neotethys to the west as argued by Soares et al.

(2012), then it is already Pangaea rifting and there is no argument to say that the red siliciclastic deposits prior to Castelo Viegas do not belong to the LB. Moreover, the Castelo Viegas Formation is the proximal equivalent of the distal Hettangian evaporites (Soares et al., 2012; Vilas-Boas et al., 2021), which means that Soares et al. (2012) suggested that the LB started in the Hettangian, i.e. ca. 200 Ma ago, with the evaporites. This idea contradicts all previous literature on the LB, and the typical evolution of a continental rift, in which the evaporites appear in a second rifting stage, when restricted sea water circulation invades the rift as in the East African Rift. Soares et al. (2012) further suggested the existence of a "proto-Lusitanian Basin" forming at ca. 245 Ma (earliest Middle Triassic), which is not supported by the well-established ages of the Silves Group.

4.2. Meaning of the structural data

Angelier (1989) established that, when using the right dihedra method to infer the palaeostress field, the α angle should be maintained under 22º for the method to be accurate. In our case, to comply with this condition, it would be necessary to exclude 83% of the faults, otherwise the uncertainty is greatly increased (Fig. 6B). This may have two explanations: (1) the measured faults were not all of them produced by the same stress field, or (2) the measured faults result from reactivation of inherited faults.

The meaning of the measured structural data is not straightforward, because fault-plane lineations can be misleading and most faults follow inherited trends, which means that stress inference from fault data can be erroneous. Striations in coarse sandstone or conglomerate, as in the studied sediments, are rarely produced and even less preserved. The lineation observed on the fault plane is commonly an intersection lineation that results from the intersection of crossbedding with the fault plane. Therefore, in this discussion we will discard the measured "striations", and will analyse what striations are expected to form during E-W extension affecting inherited fault planes oriented NNE-SSW, ENE-WSW and NW-SE. The significant dispersion observed in fault orientation (cf. Fig. 8), and the fact that they are observed within the sediments, hints that part of the faults may have been produced by differential compaction (Carminati et al., 2010; Berra and Carminati, 2012). Also, the dip of the measured faults is greater than the typical normal fault dip, suggesting that most faults are not pure normal faults (mixed normal and strike-slip motions).

Comparison between measured faults (Figs. 6A and 7A) and the Variscan tectonic trend and main fault systems shows that rifting was mostly accommodated by inherited Variscan trends: NW-SE tectonic trend and NNE-SSW fault system (Marques et al., 2002). Noticeably, the ENE-WSW conjugate does not seem to have been reactivated. Our explanation for this is that $\sigma 1$ was vertical and $\sigma 3$ horizontal, and therefore the ENE-WSW fault system was not favourably oriented to be reactivated. If our inference is correct, then the opening of the LB was in the ENE-WSW direction. We also note that the fault dip is greater than the common ca. 60º, which also indicates reactivation of inherited Variscan steeply dipping strike-slip faults.

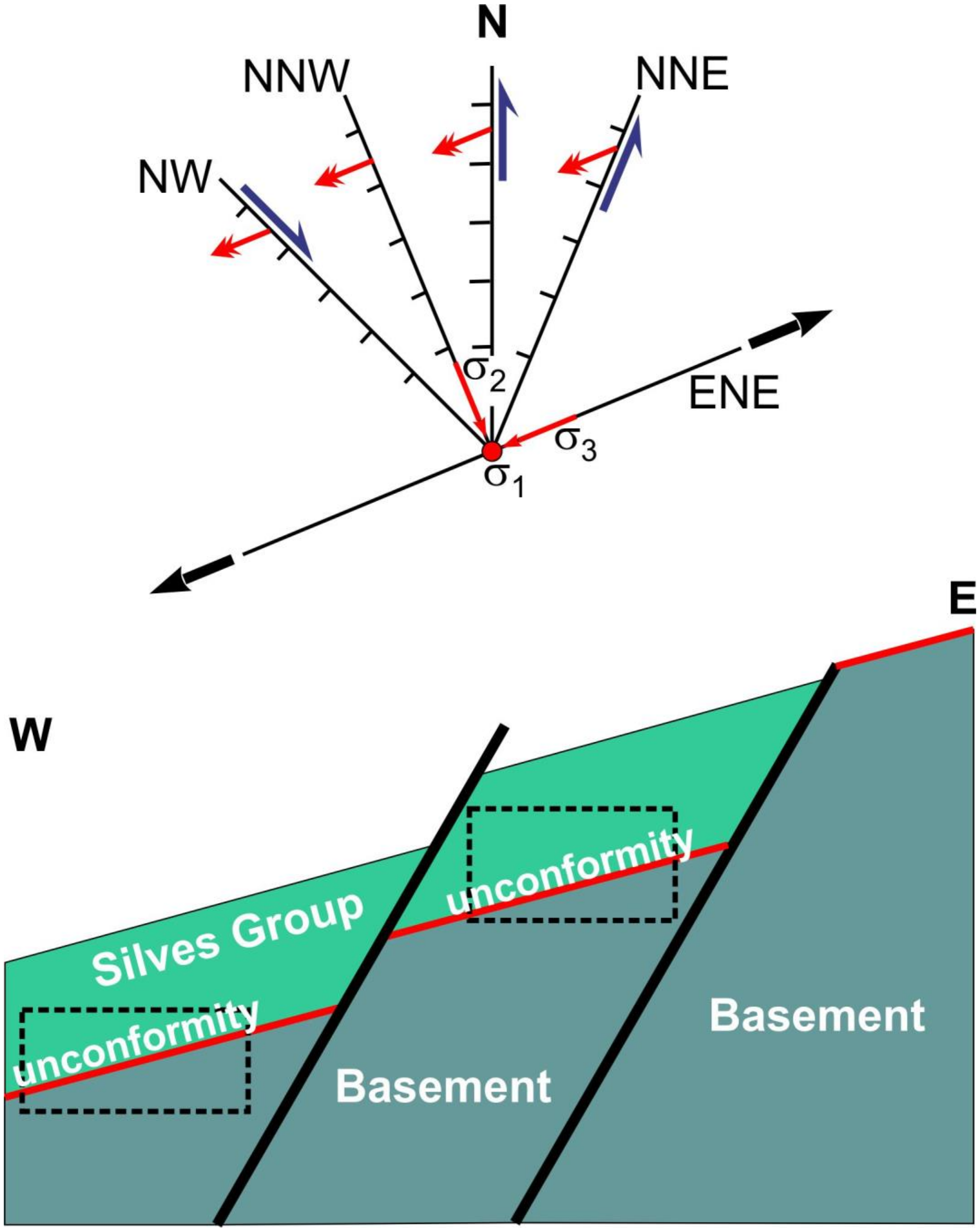

Figure 9. Top panel – schematic representation of striations (red double arrows) produced by ENE-WSW extension (black arrows) during reactivation (rifting), and respective fault kinematics (ticks and half arrows represent the normal and the strike-slip components, respectively). ENE faults have no motion during reactivation to be consistent with vertical σ1 and ENE-WSW σ3. Bottom panel – cross section showing the effects of partial observation (dashed rectangles) on the interpretation (half-graben) of the true tectonic structure (full graben).

What can we expect, in terms of striations, from ENE-WSW extension on inherited faults oriented NW-SE, NNW-SSE, NNE-SSW or ENE-WSW (Fig. 9 top panel)? On NW-SE faults the striation would be oblique, with a dextral strike-slip component. On NNW-SSE faults the striation would be dip-slip, because the fault trend is perpendicular to $\sigma 3$. On NNE-SSW faults the striation would be oblique, with a sinistral strike-slip component. The ENE-WSW fault system would not be reactivated as explained above.

Given that the topography at the rifting onset should be flat and close to sea level (Variscan topography eroded to the ground – full denudation), one would expect that one principal stress be sub-vertical and represent overburden (e.g. Lacomb, 2012). As shown in Fig. 6B, the greatest compressive stress (σ_1) is not vertical, although expected for a pure normal fault, and deviates significantly from vertical (ca. 30º). This indicates that: (1) the used approach to produce stress inversion from fault-slip data might not be appropriate for the studied faults; in fact, the used technique is for faults generated by a certain stress field, not for faults inherited from a previous tectonic cycle. (2) Non-vertical σ_1 is the result of oblique slip on inherited faults. (3) The stress inversion results confirm that faults were inherited from the Variscan orogeny.

4.3. Nature of the LB's eastern margin (flexural, faulted, or both?)

As an introduction to this section, we would like to recall the concept of rift shoulder uplift (e.g Weissel and Karner, 1989), because this upward movement of the footwall is responsible in western Iberia for providing the siliciclastic sediments that filled the LB at different stages of the rifting process. Young continental rifts, like the Red Sea and the East African rifts, show impressive uplift on both rift shoulders, reaching two to three thousand meters. If Pangaea rifting in western Iberia has undergone a similar process, then the LB should have developed as a graben bounded by tall master normal faults. Moreover, the eastern LB boundary follows two major Variscan fault trends, the NNW to N-S and the NNE, thus indicating that this boundary should be made of master faults reactivating inherited Variscan shear zones and faults. Therefore, we looked for evidence of these faults, and we found sediment/basement contacts by fault and by fault scarp. However, we also found low angle unconformable contacts of siliciclastic sediments over basement, thus hinting an initial half-graben or a pre-rift sag basin. However, what we currently observe can be deceiving, because the unconformable contacts we see between the Silves Group and underlying Variscan basement may only represent a partial view of a block actually bounded by normal faults in the east and west (Fig. 9 bottom panel). If we do not consider the fault in the east, then the structure looks like a half-graben.

Given that, in the northern two thirds of the study area the footwall is Black Schist and the clasts comprising the hanging wall are mostly of quartzite and quartz eroded from topographic highs further away to the east, the fault scarp contact between red siliciclastic sediments and basement is here interpreted in two ways: (1) erosion acting faster than tectonics, which is consistent with the slow rifting process that lasted for ca. 120 Ma, since initiation at ca. 230 Ma (e.g. Wilson et al., 1989) to final rift-to-drift at ca. 110 Ma (e.g. Driscoll et al., 1995; Barbarand et al., 2021); (2) migration of the master bounding fault to the east (this work and Barbarand et al., 2021). Barbarand et al. (2021) suggested that the initial post-Variscan basin could be wider than currently observed and bounded by two major NNE-SSW faults further to the east.

Given that we could not find a complete exposure of the sediment/basement master fault contact, this can be interpreted in two ways: (1) the master bounding fault is syn-rift, which means that the LB is a full graben and the Silves Group is also syn-rift (Upper Triassic); (2) the master bounding fault post-dates the initial rifting and displaces the sediment/basement unconformity, which could mean that the base of the Silves Group pre-dates the Upper Triassic LB rifting.

The depth-to-basement map shows two contrasting situations at the LB's eastern margin (Fig. 10): (1) bulk gentle slope (ca. 10º) SSW of Tomar, although likely made of steps produced by normal faults; (2) steeper slope (> 30º) N of Tomar through Coimbra, and WNW of Coimbra along a NNE-SSW direction. From this we infer that the gentle slopes correspond to a mixed half-graben and full graben rifting style, and that the steep slopes correspond to master faults bounding a full graben. It seems therefore that the Porto-Tomar shear zone worked as a preferential weakness for a faulted LB's eastern boundary. None of these rifting styles hinders the existence of a pre-LB sag basin.

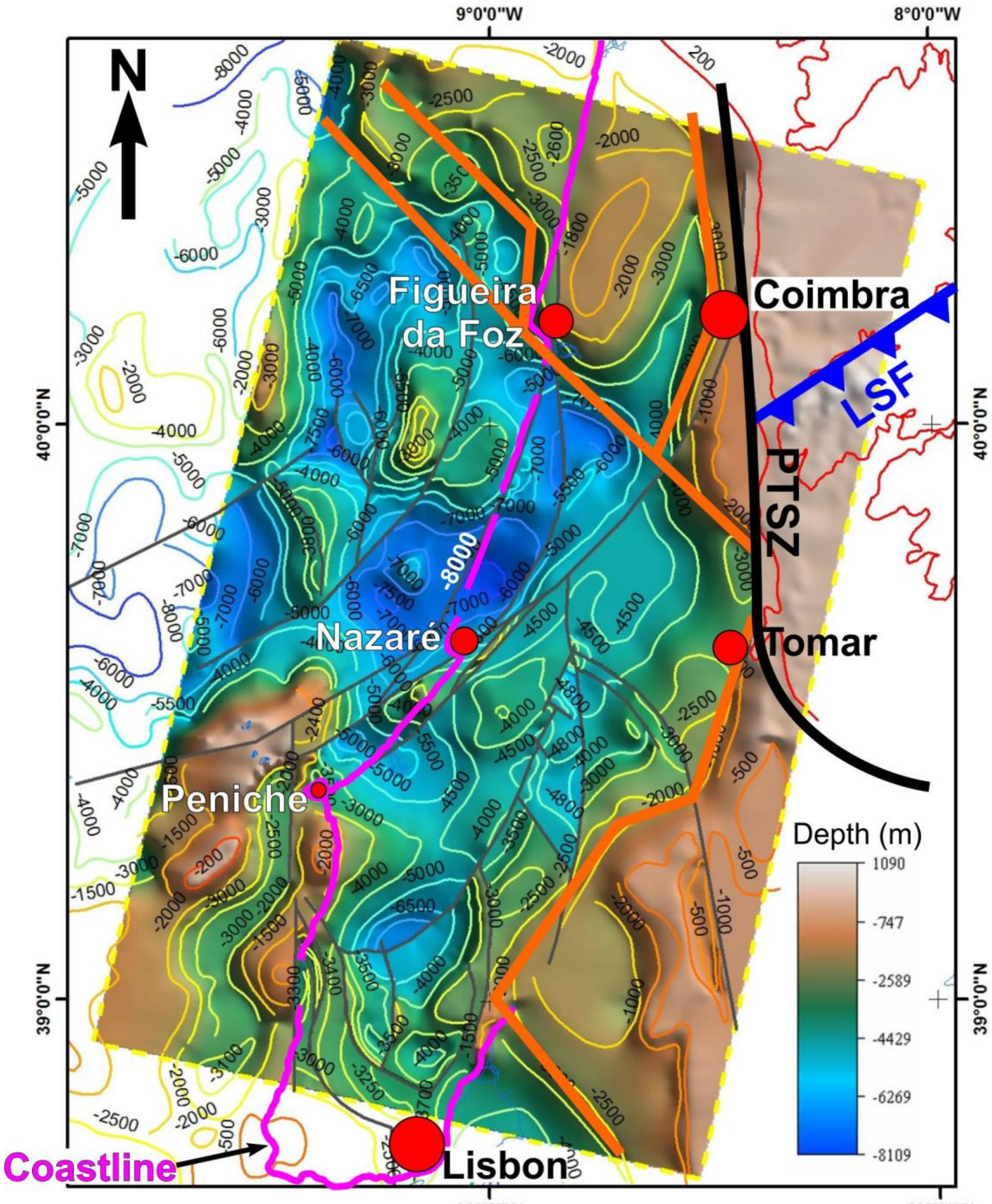

Figure 10. Depth-to-basement model produced by SEEBASE, FrOGTech, 2012. LSF – Lousã-Seia Fault bounding Serra da Estrela in the north. PTSZ – Porto-Tomar shear zone. Orange lines represent interpreted main faults.

We also collected data on the adjacent basement, hence we perceive that the rift tectonics also affected the adjacent basement significantly, because the main synsedimentary fault sets

(NW-SE and NNE-SSW) are profusely present in the basement. As also reported in previous work (e.g. Soares et al., 2012), the throw of the faults inside the Silves Group is small, typically < 1 m, and therefore the accumulated vertical displacement is also very limited, from which we infer that the main vertical displacement should be elsewhere. We found undeformed red continental deposits (Silves Group) at different altitudes (more than 50 m in one place; cf. Fig. 3N, unconformable on the Variscan basement, indicating a step-like architecture of the LB's eastern boundary. In the basement to the east of the LB, major NNE-SSW faults can be observed, which might have worked as master bounding faults of the Mesozoic rift. This rifting to the east of the current exposure of the Silves Group was also inferred by Barbarand et al. (2021) using AFT cooling ages.

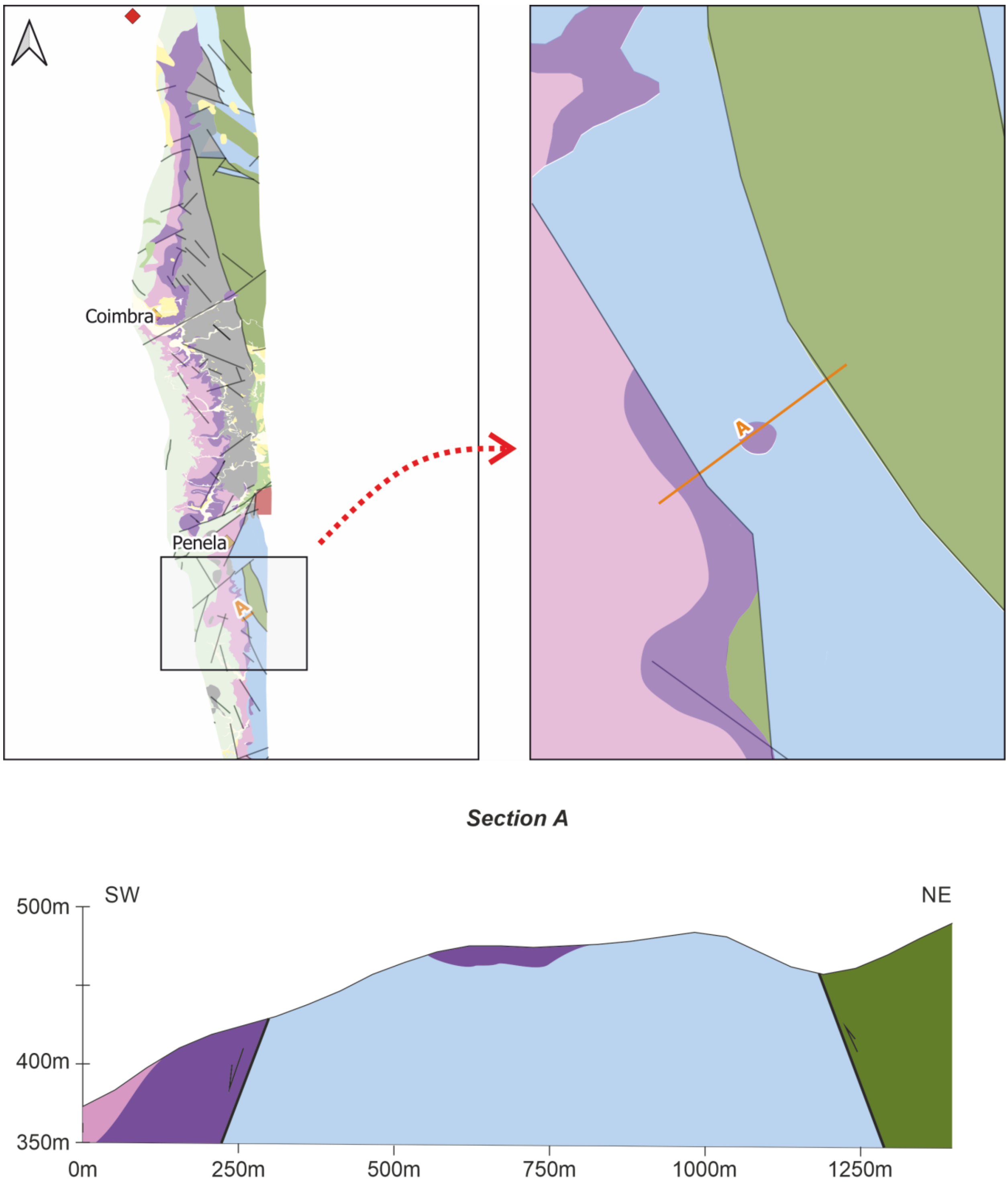

Figure 11: Detailed cross-section where the Conraria Fm. was found lying, undeformed, over the basement through an angular unconformity to the southeast, and through normal fault to the northwest.

Here we argue in favour of the hypothesis that the lower Conraria Formation sediments were deposited in a post-orogenic sag basin associated with the gravitational collapse of the

Variscan chain in western Iberia. Similarly, a post-orogenic extension mechanism is considered for the formation of the Iberian Basin (Arche and López-Gómez, 1996), a basin that shares the Variscan basement with the LB. Therefore, the Arche and López-Gómez (1996) reasoning for the Iberian Basin can be effectively modified and applied to the basin formation in the western margin of Iberia:

(1) The Variscan orogeny resulted in the shortening and thickening of the crust up to 60 km (Arche and López-Gómez, 1996). High topographic relief and thick crust are stable as long as tectonic compression exists to support topography and thick low-density roots. If compression ceases, then gravitational collapse and elastic rebound take place (e.g. Rey et al., 2001).

(2) Significant weakening of the crust occurs typically after 15 to 20 Ma of the main orogenic event, when the base of the crust begins to delaminate and collapse (Arche and López-Gómez, 1996).

(3) Delamination leads to rapid uplift of the crust, accompanied by increased geothermal gradient, resulting, typically after 30 to 35 Ma, in thermal subsidence (Arche and López-Gómez, 1996).

The above reasoning can explain the formation of a post-orogenic sedimentary basin 45 to 55 Ma after the end of the Variscan compressional tectonics, which should be coincident with the deformation of the Buçaco Basin sediments at ca. 300 Ma (Machado et al., 2018). This points toward basin formation at about 250 Ma, before the deposition of the upper Conraria Formation dated at ca. 220-207 Ma (Vilas-Boas et al., 2021).

The formation of a post-orogenic basin related to an orogenic collapse instead of a classical rifting process in the Permian or Triassic could explain the absence of volcanism in the eastern LB. The gravitational collapse of the continental crust tends to generate shallow structures and limit the thinning of the lithosphere, especially in its early stages (Rey et al., 2001). This fact added to the thickness of the crust in the central Iberian Massif (Arche and López-Gómez, 1996; Díaz and Gallart, 2009) could have hindered the production of magma.

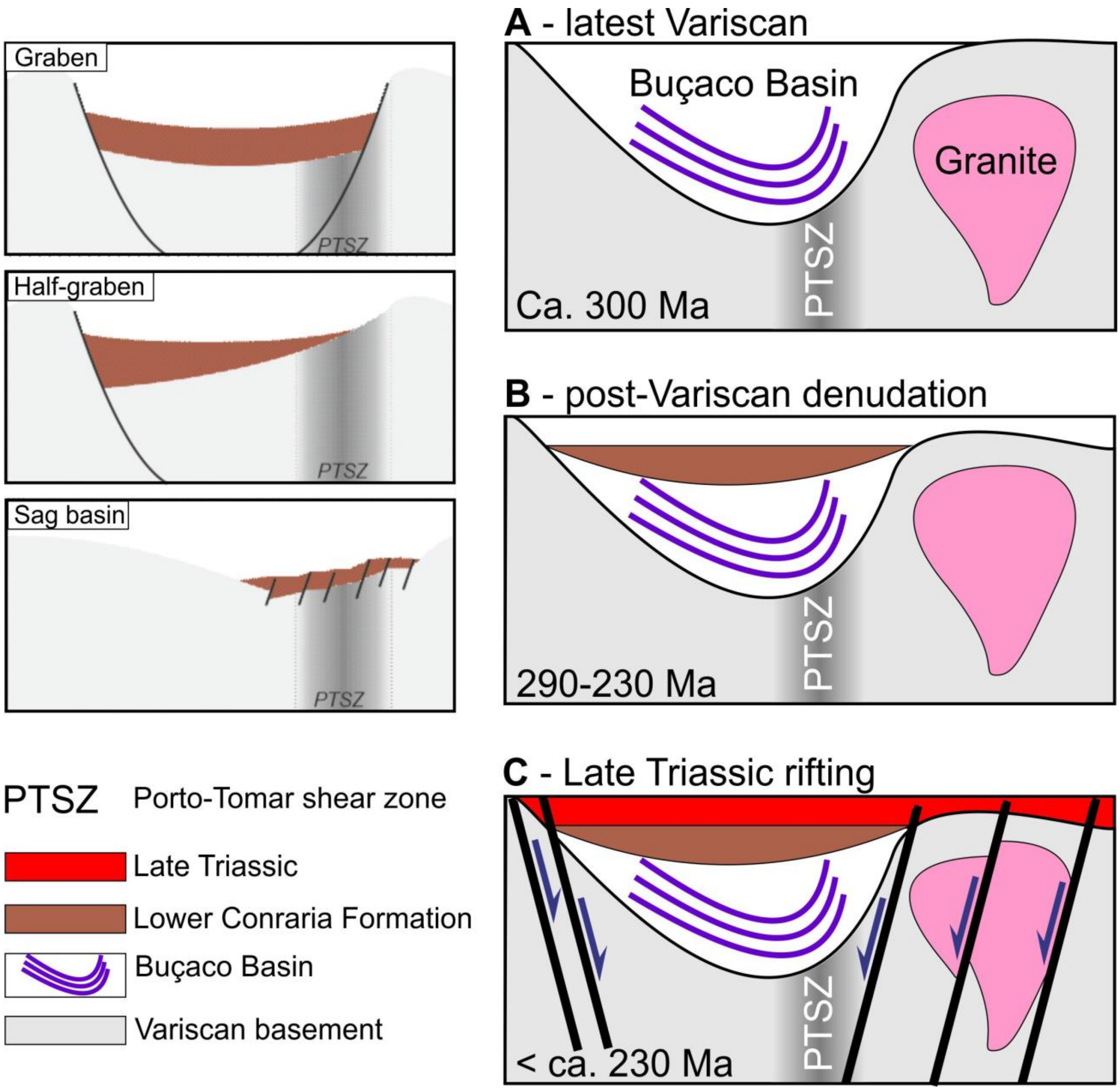

Figure 11. Left panel – sketches of three possible types of basin representing the Lusitanian Basin or its predecessors: top – graben (bounded by master faults); middle – half-graben (flexural on one side, and bounded by master fault on the other); bottom – intracratonic sag basin (no master bounding faults, but possible minor faults). Right panel – tectonic evolution of western Iberia from Late Carboniferous/Permian to Late Triassic showing late-Variscan sediment deposition in intramountain basins and their deformation (A), post-Variscan orogenic collapse and denudation (B) and Late Triassic rifting at the onset of the Lusitanian Basin. Deformation of the Buçaco sediments may be due to the intrusion of large granitic bodies at this age.

5. Conclusion

The eastern border of the LB comprises two contrasting types of contact between red sediments and Variscan basement: major angular unconformity and master bounding fault. The unconformable contact could mean a pre-rift sag basin, or a syn-rift half-graben with flexural boundary in the E. However, given that newly recognized master NW-SE to NNW-SSE bounding faults displace the red continental deposits and basal unconformity by hundreds of meters, we infer that the master bounding fault is Alpine and displaces the base of a previous sag basin. Moreover, the unconformable red sediments were deposited in debris-flow dominated fans, indicating that the topography was low, consistent with a sag basin. In the case of unconformable contact and sag basin, the age of the red continental deposits would be older than the currently attributed Late Triassic age. Given that we found master bounding faults east of the Porto-Tomar Shear Zone in the Coimbra region, we do not consider the half-graben hypothesis, at least north of Tomar (cf. Fig. 10). From the geophysical data (Fig. 10), it is possible that south of Tomar there is a mixture of half-graben and full graben, because some major faulting can still be interpreted.

From previous work and data reported here, we can summarize the following evolution of the western Iberian margin in the period 300 to 190 Ma (Fig. 11 right hand panel):

(A) Late-Variscan stage – In the Late Carboniferous to Early Permian (ca. 300 Ma), the Buçaco intramountain basin formed in angular unconformity over deformed and eroded basement. The Buçaco sediments were deformed shortly after, likely by intrusion of large granitic bodies (Fig. 11A right panel). According to Solá et al. (2009), Lopes et al. (2016) and Neiva et al. (2012), the U-PB zircon age of intrusion of post-tectonic granites occurred around 305-300 Ma, and were exhumed relatively fast between 300 and 285 Ma (Hildenbrand et al., 2021).

(B) Orogenic collapse and denudation – In the period ca. 300-285 Ma, feldspars of three samples in Hildenbrand et al. (2021) show relatively rapid cooling (12–25 ºC/Ma), corresponding to relatively fast exhumation (300–600 m/Ma). Between ca. 285 and 275 Ma, the granites sampled by Hildenbrand et al. (2021) experienced modest cooling and exhumation (5 to 8 ºC/Ma, corresponding to 1 to 2 km uplift), likely due to denudation and isostatic rebound.

From ca. 275 to 250 Ma, most granitic samples in Hildenbrand et al. (2021) remained at shallow depth. At the late stages of this period, or immediately after, sag basins may have formed that were filled by the red sediments comprising the lower 120 m of the Conraria Formation. The location of these sag basins seems to have been controlled by main structures in the Variscan basement, e.g. the Porto-Tomar Shear Zone.

(C) Late Triassic rifting – At ca. 220 Ma, deposition of the upper half of the Conraria Formation started. In our view, this is the age of rifting initiation that corresponds to the onset of the Alpine cycle in the Newfoundland-Iberia rift.

A similar development of composite basins can be found in NE Brazil, where some Mesozoic intracontinental basins also show evidence of two-stage basin formation: (1) an older (Devonian; Silva et al., 2014) sag basin sits unconformably on Brasiliano basement through a major erosion surface that exposes rocks older than 500 Ma; (2) in the Cretaceous, the Devonian sag basin was juxtaposed by a rift basin (e.g. Vasconcelos et al., 2021). Similarly to western Iberia, the basins in NE Brazil are also bounded by master faults that have reactivated main structural trends in the basement (Matos, 1992; Gurgel et al., 2013; Marques et al., 2014; Nogueira et al., 2015; Vasconcelos et al., 2021; Ramos et al., 2022).

Acknowledgments

This work was supported by FAPERJ, Brazil. DG benefited from a CNPq Ph.D exchange program (SWE).

Data availability statement

All the data we used in this study is included in this manuscript.

References

Adloff, M.C., Doubinger, J., Palain, C., 1974. Contribution à la palynologie du Trias et du Lias de Portugal. Comunicações dos Serviços Geológicos de Portugal 58, 91-114.

Alves, T. M., Gawthorpe, R. L., Hunt, D. W., & Monteiro, J. H. (2002). Jurassic tectono-sedimentary evolution of the Northern Lusitanian Basin (offshore Portugal). Marine and Petroleum Geology, 19(6), 727-754.

Alves, T.M., Moita, C., Cunha, T., Ullnaess, M., Myklebust, R., Monteiro, J.H., Manuppella, G. 2009. Diachronous evolution of Late Jurassic–Cretaceous continental rifting in the northeast Atlantic (west Iberian margin). Tectonics 28, TC4003, doi: 10.1029/2008TC002337.

Angelier, J., 1989. From orientation to magnitudes in paleostress determinations using fault slip data. Journal of Structural Geology, 11(1), 37-50.

Angelier, J., 1994. Fault slip analysis and paleostress reconstruction. Continental deformation, 4.

Angelier J., Mechler P., 1977. Sur une méthode graphique de recherche des contraintes principales également utilisable en tectonique et en séismologie: la méthode des dièdres droits. Bull. Soc. géol. France, (7), XIX, 6, p. 1309-1318.

Arche, A., López-Gómez, J., 1996. Origin of the Permian-Triassic Iberian Basin, central-eastern Spain. Tectonophysics 266, 443-464.

Arche, A., López-Gómez, J., 2014. The Carnian Pluvial Event in Western Europe: new data from Iberia and correlation with the Western Neotethys and Eastern North America–NW Africa regions. Earth-Sci. Rev. 128, 196–231.

Arthaud, F. & Matte, P. (1975). Les décrochements Tardi-Hercyniens du Sud-ouest de l'Europe. Géometrie et essai de reconstitution des conditions de la déformation. Tectonophysics 25, 139–171.

Arthaud, F. & Matte, P. (1977). Late Paleozoic strike-slip faulting in southern Europe and northern Africa - result of a right-lateral shear zone between Appalachians and Urals. Geological Society of America Bulletin 88, 1305-1320.

Azeredo, A. C., Duarte, L. V., Henriques, M. H., Manuppella, G. (2003). Da dinâmica continental no Triásico aos mares do Jurássico Inferior e Médio. Cadernos de Geologia de Portugal 54 pp.

Barbarand, J., Marques, F. O., Hildenbrand, A., Pinna Jamme, R., Nogueira, C.R., 2021. Thermal evolution of onshore west Iberia: a better understanding of the ages of breakup and rift-to-drift in the Iberia-Newfoundland Rift. Tectonophysics 813, 228926 https://doi.org/10.1016/j.tecto.2021.228926.

Berra, F., Carminati, E., 2012. Differential compaction and early rock fracturing in high-relief carbonate platforms: numerical modelling of a Triassic case study (Esino Limestone, Central Southern Alps, Italy). Basin Research 24, 598–614.

Carminati E., Scrocca, D., Doglioni, C. 2010. Compaction-induced stress variations with depth in an active anticline: Northern Apennines, Italy. Journal Geophysical Research 115, doi: 10.1029/2009JB006395.

Choffat, P. (1882). Note sur les vallées tiphoniques et les eruptions d'ophite et de teschenites en Portugal. Bull. Soc. Géol. France 3e sér.,X, 267-295, Paris.

Choffat, P. (1903-1904). L'Infralias et le Sinémurien au Portugal. Com. Serv. Geol. Portugal V, 49-114, Lisboa.

Dallmeyer, R. D., Martínez Catalán, J. R., Arenas, R., Gil Ibarguchi, J. I., Farias, P., Bastida, F., & Aller, J. (1997). Diachronous Variscan tectonothermal activity in the NW Iberian Massif: Evidence from $^{40}Ar/^{39}Ar$ dating of regional fabrics. Tectonophysics, 277(4), 307-337.

Delvaux, D. (2012). Release of program Win-Tensor 4.0 for tectonic stress inversion: statistical expression of stress parameters. In EGU General Assembly Conference Abstracts, vol. 14, p. 5899.

Dias, G., Leterrier, J., Mendes, A., Simões, P.P., Bertrand, J.M., 1998. U-Pb zircon and monazite geochronology of post-collisional Hercynian granitoids from the Central Iberian Zone (Northern Portugal). Lithos 45, 349–369.

Díaz, J., Gallart, J., 2009. Crustal structure beneath the Iberian Peninsula and surrounding waters: A new compilation of deep seismic sounding results. Physics of the Earth and Planetary Interiors 173, 181-190.

Díez, J.B., 2000. Geologia y Paleobotanica de la Facies Buntsandstein en la Rama Aragonesa de la Cordillera Iberica, Implicaciones bioestratigraficas en el Peritethys Occidental. Univ. de Zaragoza/Univ. Pierre et Marie Curie-Paris-6, unpublished PhD Thesis.

Domingos, L.C.G., Freire, J.L.S., Gomes da Silva, F., Gonçalves, F., Pereira, E., Ribeiro, A., 1983. The structure of the intramontane upper Carboniferous basins in Portugal. Memórias dos Serviços Geológicos de Portugal 29, 187–194.

Doubinger, J., Adloff, M., Palain, C., 1970. Nouvelles précisions stratigraphiques sur la série de base du Mésozoïque portugais. Extr. Comptes rendus des séances de l’Académie des Sciences de Paris 270, 1170-1172.

Driscoll, N.W., Hogg, J.R., Christie-Blick, N., Karner, G.D., 1995. Extensional tectonics in the Jeanne d’Arc Basin, offshore Newfoundland: implications for the timing of break-up between Grand Banks and Iberia. In: Scrutton, R.A., Stoker, M.S., Shimmield, G.B., Tudhope, A.W. (Eds.), The Tectonics, Sedimentation and Palaeogeography of the North Atlantic Region.

Geological Society Special Publication, London, pp. 1–28.

Einsele, G., 2000. Sedimentary Basins – Evolution, Facies and Sedimentary Budget, Springer, New York, p. 729.

FrOGTech, 2012. Report compiled for Mohave Oil and Gas Corporation.

Gurgel, S.P.P., Bezerra, F.H.R., Corrêa, A.C.B., Marques, F.O., Maia, R.P., 2013. Cenozoic uplift and erosion of structural landforms in NE Brazil. Geomorphology 186, 68-84.

Kullberg, J. C., Rocha, R. B., Soares, A. F., Rey, J., Terrinha, P., Callapez, P., & Martins, L. 2006. A Bacia Lusitaniana: estratigrafia, paleogeografia e tectónica. In: Geologia de Portugal no contexto da Ibéria (R. Dias, A. Araújo, P. Terrinha & J. C. Kullberg, Eds.). Univ. Évora, pp. 317-368.

Machado, G., Vavrdová, M., Fonseca, M., Fonseca, P.E., Rocha, F., 2018. Stratigraphy and palynology of the Pennsylvanian continental Buçaco Basin (NW Iberia). Geobios 51, 507-516.

Marques, F.O., Mateus, A., Tassinari, C., 2002. The Late-Variscan fault network in central-northern Portugal (NW Iberia): a re-evaluation. Tectonophysics 359, 255-270.

Marques, F.O., Nogueira, C.R., 2008. Normal fault inversion by orthogonal compression: Sandbox experiments with weak faults. Journal of Structural Geology 30, 761–766.

Marques, F.O., Nogueira, F.C.C., Bezerra, F.H.R., de Castro, D.L., 2014. The Araripe Basin in NE Brazil: An intracontinental graben inverted to a high-standing horst. Tectonophysics 630, 251-264.

Martínez Catalán, J.R., 2011. Are the oroclines of the Variscan belt related to late Variscan strike-slip tectonics?. Terra Nova 23, 241-247.

Martínez Catalán, J.R., Rubio Pascual, F.J., Montes, A.D., Fernández, R.D., Barreiro, J.G., Dias Da Silva, Í., Clavijo, E.G., Ayarza, P., Alcock, J.E., 2014. The late Variscan HT/LP metamorphic event in NW and Central Iberia: relationships to crustal thickening, extension, orocline development and crustal evolution. Geological Society London, Special Publications

405, 225–247.
Miall, A.D., 1996. The geology of fluvial deposits: sedimentary facies, basin analysis and petroleum geology. Springer-Verlag Inc., Berlin, 582 pp..
Middleton, M.F., 1989. A model for the formation of intracratonic sag basins. Geophysical Journal International 99, 665–676. doi:10.1111/j.1365-246x.1989.tb02049.x
Neiva, A.M.R., Williams, I.S., Lima, S.M., Teixeira, R.J.S., 2012. U–Pb and 39Ar/40Ar data constraining the ages of the source, emplacement and recrystallization/cooling events from late- to post-D3 Variscan granites of the Gouveia area, central Portugal. Lithos 153, 72-83.
Nogueira, F.C.C., Marques, F.O., Bezerra, F.H.R., de Castro, D.L., Fuck, R.A., 2015. Cretaceous intracontinental rifting and post-rift inversion in NE Brazil: insights from the Rio do Peixe Basin. Tectonophysics 644-645, 92-107.
Oliveira, J.P., Pereira, E., Ramalho, M. M., Antunes, M. T., Monteiro, J. H., 1992. Carta Geológica de Portugal, escala 1/500.000. Serv. Geol. Portugal, Lisboa.
Palain, C., 1976. Une série détritique terrigène. Les "Grès de Silves": Trias et Lias inférieur du Portugal. Mem. Serv. Geol. Portugal 25, 377 p.p., Lisboa, Portugal.
Pena dos Reis, R., Pimentel, N., Garcia, A., 2010. A evolução da Bacia Lusitânica (Portugal) e dos sistemas petrolíferos associados. VIII CNG 2010, 19.
Ramos, G.V., Vasconcelos, D.L., Marques, F.O., Castro, D.L., Nogueira, F.C.C., Bezerra, F.H.R., Perez, Y.A.R., Souza, J.A.B., Medeiros, V.C., 2022. Relations between inherited basement fabric and fault nucleation in a continental setting: the Rio do Peixe Basin, NE Brazil. Marine and Petroleum Geology, 139, 105635. DOI: 10.1016/j.marpetgeo.2022.105635.
Rasmussen, E. S., Lomholt, S., Andersen, C., Vejbæk, O. V., 1998. Aspects of the structural evolution of the Lusitanian Basin in Portugal and the shelf and slope area offshore Portugal. Tectonophysics, 300(1), 199-225.
Rey, P., Vanderhaeghe, O., Teyssier, C., 2001. Gravitational collapse of the continental crust:

definition, regimes and modes. Tectonophysics 342, 435-449.

Silva, J. G. F., Córdoba, V. C., & Caldas, L. H. C. (2014). Proposta de novas unidades litoestratigráficas para o Devoniano da Bacia do Rio do Peixe, Nordeste do Brasil. Brazilian Journal of Geology, 44(4), 561–578. https://doi.org/10.5327/Z2317 48892 01400 040004

Soares, A.F., Kullberg, J.C., Marques J.F., Rocha, R.B. & Callapez. P., 2012. Tectono-sedimentary model for the evolution of the Silves Group (Triassic, Lusitanian Basin, Portugal). Bull. Soc. Géol. France, 183: 203-216.

Soares, A.F., Marques, J. F., Sequeira, A., 2007. Carta geológica de Portugal e Notícia Explicativa da Folha 19D (Coimbra-Lousã), na escala 1;50000. INETI, Lisboa. 71 pp..

Tucholke, B.E., Sibuet, J.C., 2007. Leg 210 synthesis: tectonic, magmatic, and sedimentary evolution of the Newfoundland-Iberia rifte. In Tucholke, B.E., Sibuet, J.-C., and Klaus, A. (Eds.), Proc. ODP, Sci. Results, 210: College Station, TX (Ocean Drilling Program), 1–56.

Uphoff, T.L., 2005. Subsalt (pre-Jurassic) exploration play in the northern Lusitanian basin of Portugal. AAPG bulletin 89, 699-714.

Valle Aguado, B., Azevedo, M.R., Nolan, J., Medina, J., Costa, M.M., Corfu, F., Martínez Catalán, J.R., 2017. Granite emplacement at the termination of a major Variscan transcurrent shear zone: The late collisional Viseu batholith. Journal of Structural Geology 98, 15-37.

Vasconcelos, D.L., Marques, F.O., Nogueira, F.C.C., Perez, Y.A.R., Bezerra, F.H.R., Stohler, R.C., Souza, J.A.B., 2021. Tectonic inversion assessed by integration of geological and geophysical data: the intracontinental Rio do Peixe Basin, NE Brazil. Basin Research 33, 705-728. 10.1111/bre.12491.

Vilas-Boas, M., Pereira, Z., Cirilli, S., Duarte, L.V., Fernandes, P., 2021. New data on the palynology of the Triassic–Jurassic boundary of the Silves Group, Lusitanian Basin, Portugal. Rev. Palaeobot. Palyn. 290, 104426, https://doi.org/10.1016/j.revpalbo.2021.104426

Weissel, J.K., Karner, G.D., 1989. Flexural uplift of rift flanks due to mechanical unloading of the lithosphere during extension, J. Geophys. Res. 94, 13919-13950.

Wilson, R. C. L., Hiscott, R. N., Willis, M. G., Gradstein, F. M., 1989. The Lusitanian Basin of west-central Portugal: Mesozoic and Tertiary tectonic, stratigraphic, and subsidence history. Extensional tectonics and stratigraphy of the North Atlantic margins 46, 341-361.